solids

MDPI

Article

Reheating and Roller Forming of Aluminum Foam Fabricated by Foaming Precursor

Yoshihiko Hangai [1,*], Kentaro Ishiuchi [1], Kenji Amagai [1] and Nobuhiro Yoshikawa [2]

[1] Graduate School of Science and Technology, Gunma University, Kiryu 376-8515, Japan
[2] Institute of Industrial Science, The University of Tokyo, Tokyo 153-8505, Japan
* Correspondence: hanhan@gunma-u.ac.jp

Abstract

Aluminum foam is expected to be applied in various industrial fields as a lightweight, multifunctional material. When it is used as an industrial product, it is essential to form it into the required shape. There have been some attempts to form aluminum foam. However, the formability remains low. In this study, we attempted to form aluminum foam, which was fabricated by heat foaming a precursor, into a flat plate by reheating it above its foaming temperature and then roller forming it. It was found that heating above the foaming temperature and subsequent roller forming enabled the aluminum foam to be formed into a flat plate without causing defects. In a sample in which the precursor was roller-formed immediately after foaming, it was found that compared to the as-foamed aluminum foam, the decrease in porosity was limited to approximately 5%, enabling roller forming while minimizing the influences on pore structures. In samples that were roller-formed after reheating, porosities slightly decreased, but most pores were retained. Even when the aluminum foam was roller-formed to the same thickness as the initial precursor before foaming, the porosities exhibited around 65%, limiting the reduction in porosities to approximately 15% compared to the as-foamed aluminum foam.

Keywords: porous aluminum; aluminum foam; roller forming; reheating; precursor; optical heating

1. Introduction

Aluminum foam is a lightweight aluminum material containing numerous pores [1,2]. Due to the existence of numerous pores, it exhibits excellent shock absorption, sound insulation, and thermal insulation properties. Therefore, as a lightweight, multifunctional material, it is expected to be applied in various fields such as automotive components and building materials [3–5]. With the current demand for reducing CO_2 emissions, lightweight materials based on aluminum, which have excellent recyclability [6,7], are expected to increase their use in the future.

When aluminum foam is used as an industrial product, it is essential to form it into the required shape. Aluminum foam is a difficult material to form because it consists of numerous pores with thin aluminum cell walls. There have been some attempts to form aluminum foam, including laser forming [8–11], compression forming [12–15], bulge forming [16,17], incremental forming [18,19], and extrusion and rolling [20,21], but the formability remains low. For example, in the case of forming by bending deformation, thin cell walls fracture on the tension side and pores collapse on the compression side, preventing the introduction of large deformation.

Check for updates

Academic Editor: Jingjing (Jenny) Qiu

Received: 8 January 2026
Revised: 5 February 2026
Accepted: 24 February 2026
Published: 2 March 2026

Copyright: © 2026 by the authors. Licensee MDPI, Basel, Switzerland. This article is an open access article distributed under the terms and conditions of the Creative Commons Attribution (CC BY) license.

Several methods for fabricating aluminum foam have been proposed, including the melt foaming process, gas injection process, spacer process, and precursor foaming process [22–26]. Among these, the precursor foaming process [27–29] is a relatively easy fabrication process for pore control due to its short heating time. This method involves preparing a precursor by mixing a foaming agent into aluminum and then heating it. The foaming agent thermally decomposes to generate gas, which forms pores in the melted aluminum and causes foaming. In this precursor foaming process, it is known that by placing the precursors into the mold and heating it, aluminum foam with the mold shape can be fabricated [29–31]. However, since the entire mold is heated, energy consumption becomes high. In addition, due to the high thermal capacity of the mold, controlling the precursor temperature is difficult. Therefore, insufficient foaming or excessive foaming easily occurs, which makes it difficult to control pore structures.

It is known that the precursor begins to foam gradually when the base aluminum is in a solid–liquid coexistence state, and then foams rapidly and significantly once the temperature exceeds the liquidus temperature [32,33]. Recently, it has been demonstrated that by press forming [34–36] or roller forming [37] immediately after the foaming of the precursor, with the aluminum foam still above the liquidus temperature, material flow occurs while maintaining pores, enabling forming. Immediately after foaming of the precursor, the base aluminum alloy is in a melt state, allowing the pores to prevent collapse due to gas internal pressure and facilitate material flow. Based on these results, it is expected that even aluminum foam that has already been foamed and is at room temperature can be formed while maintaining its pores by reheating it above its liquidus temperature. There have been several studies attempting to form aluminum foam by heating and softening. Liu et al. [38,39] attempted to form aluminum foam into a spherical crown under a solid–liquid coexistence state and found that an appropriate temperature exists. Furthermore, Movahedi et al. [40] found that in high-temperature compression tests of aluminum foam, the pores were compressed without significant collapse, exhibiting ductile behavior. However, few studies have attempted forming by heating aluminum foam above the liquidus temperature and applying significant deformation.

Therefore, in this study, we attempted to fabricate flat plates by reheating aluminum foam, which was prepared by heating and foaming a precursor to a temperature above its liquidus temperature, followed by roller forming. We also attempted to perform roller forming immediately after foaming the precursor. In addition, repeated reheating and cooling cycles of aluminum foam were performed. From these experiments, the effect of reheating on the pore structures and formability of aluminum foam was investigated.

2. Materials and Methods

2.1. Precursor Preparation

In this study, precursors were fabricated by a method utilizing friction stir welding (FSW) [41–47]. Figure 1 shows a schematic diagram of the precursor fabrication process. As shown in Figure 1a, two Al-Si-Cu aluminum alloy ADC12 [48,49] die-casting plates (210 mm × 80 mm × 3 mm) were used as the base material. Titanium hydride (TiH_2) powder (particle size less than 45 μm) was used as the foaming agent, and alumina (α-Al_2O_3) powder (particle size approximately 1 μm) as a pore structure stabilizer. After mixing the powders, they were placed between two ADC12 plates aligned with the stirring area (170 mm × 20 mm) by the FSW tool. The powder quantities were set at 1 mass% TiH_2 and 5 mass% Al_2O_3, relative to the mass of the stirred region. Subsequently, as shown in Figure 1b, the rotating tool was plunged into the stacked ADC12 plates and traversed to join the two ADC12 plates. The significant material flow generated by the tool traverse also mixed the powders into the ADC12 plates. The FSW conditions were set at a tool

rotating speed of 1200 rpm, a tool traversing speed of 120 mm/min, and a tilt angle of 3°, with the tool traversing in four rows. The four-row traverse was performed to fabricate wide-width precursors. To ensure thorough mixing of the powders, this four-row traverse was repeated a total of four times over the same area. These conditions were set with reference to ref. [50]. Subsequently, as shown in Figure 1c, a precursor with dimensions of 30 mm × 15 mm × 6 mm was cut out from the stirred region.

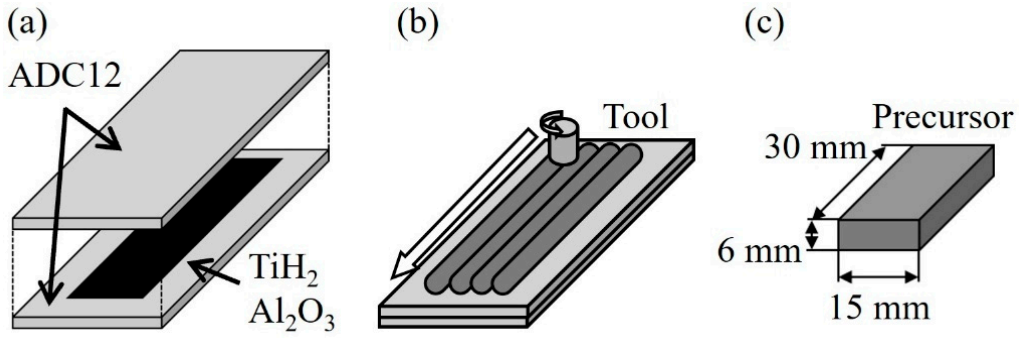


Figure 1. Schematic of the fabrication of the precursor by FSW: (**a**,**b**) FSW and (**c**) obtained the precursor.

2.2. Heat Foaming and Roller Forming

Figure 2 shows a schematic diagram of the foaming of the precursor, followed by the reheating and roller forming of the obtained aluminum foam. First, the foaming of the precursor was performed by placing the precursor on a ceramic honeycomb plate, as shown in Figure 2a, and heating it from above using a spot heater with a halogen lamp. The power consumption of the spot heater was set to 1600 W. A 3 mm deep hole was drilled in the center of the bottom of the precursor, into which a thermocouple was inserted to measure the temperature of the precursor during heating. The precursor began foaming when it was heated above the solidus temperature and expanded to a sufficient size when heated to the liquidus temperature [32,33]. The solidus and liquidus temperatures of ADC12 are 515 °C and 580 °C, respectively [51]. As shown in Figure 2b, heating was stopped when the precursor foamed and reached 630 °C, sufficiently exceeding the liquidus temperature of ADC12, and then the sample was cooled to room temperature. Figure 2c shows the reheating of the obtained aluminum foam. Heating was performed using the same spot heater as in Figure 2a, and heating was stopped at 630 °C. The temperature was measured by inserting the thermocouple into the hole used during foaming. The temperature increased to approximately 660 °C due to residual heat. When the temperature returned to 630 °C, roller forming was commenced, as shown in Figure 2d. Roller forming was performed over a distance of 60 mm, and it traversed in approximately 1.5 s. During roller forming, if the indentation depth was too high, the aluminum foam moved along with the roller. Therefore, roller forming was performed by setting the indentation depth per pass to 2 mm, traversing horizontally for a fixed distance, as shown in Figure 2e, lowering the height of the roller by 2 mm, and repeating this process five times. This resulted in a total indentation depth of 10 mm, achieving a thickness of 6 mm, identical to the original precursor. These roller forming conditions were determined based on past research [52].

Figure 3a shows a photograph of the equipment actually used in the experiment. The precursor was placed on a ceramic honeycomb plate and heated using a halogen lamp from above. The roller forming was performed by attaching the roller to the robot arm positioned on the left. Figure 3b shows the roller used in the experiment. The roller has a diameter of 30 mm and a width of 30 mm, and is made of Al-Mg series aluminum alloy AA5056. BN spray was applied to the roller surface as a release agent to prevent the adhesion of

aluminum foam. The robot arm used was the Dobot Magician, manufactured by Dobot (Shenzhen Yuejiang Technology Co., Ltd. (Shenzhen, China)).

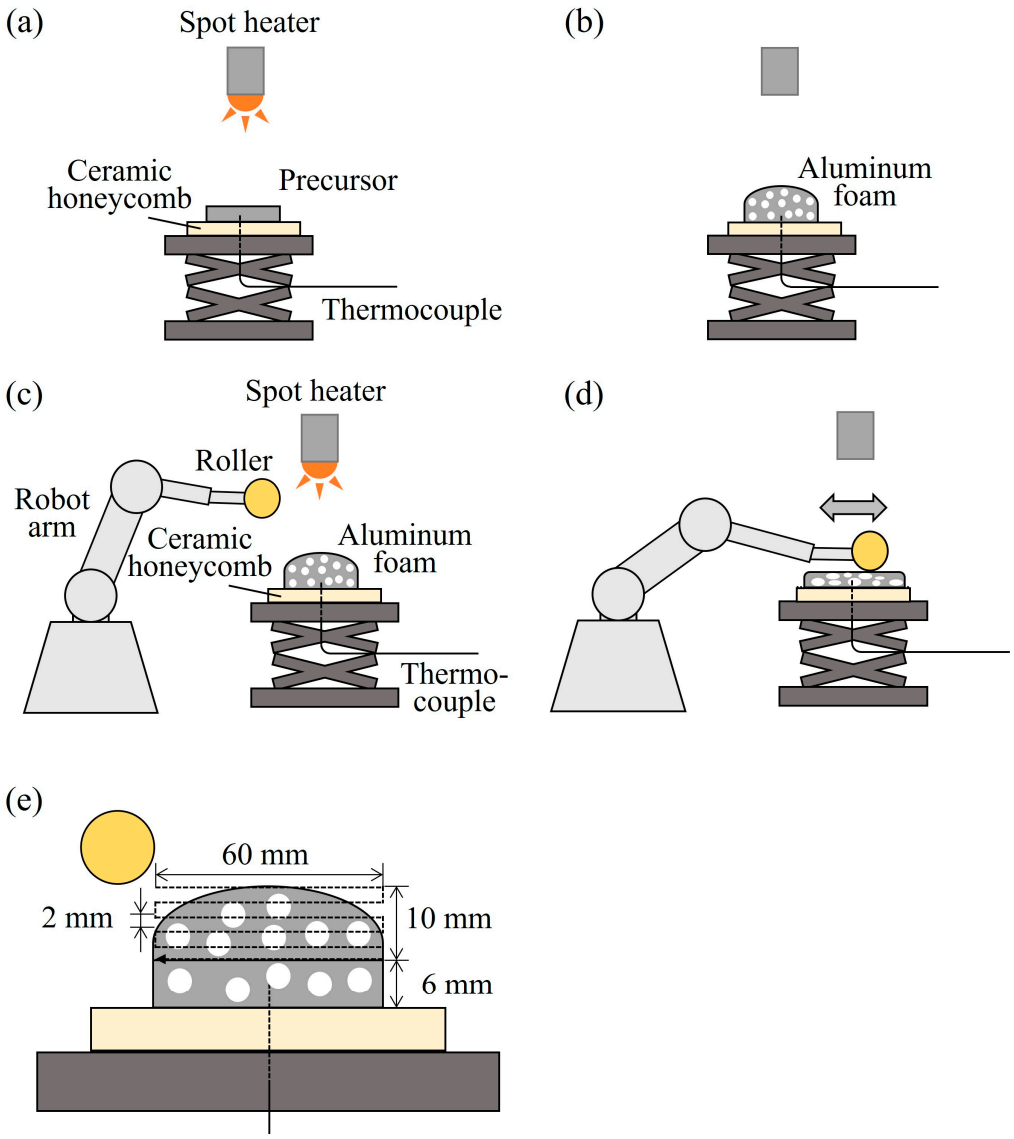


Figure 2. Schematic of experiment: (**a**) Heating precursor, (**b**) foaming and cooling, (**c**) reheating aluminum foam, and (**d**,**e**) roller forming.

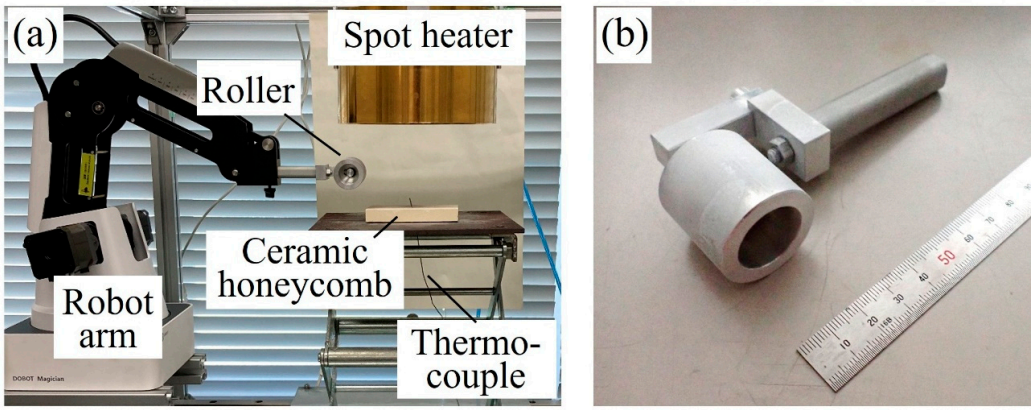


Figure 3. (**a**) Photograph of the equipment actually used in the experiment; (**b**) the roller used for forming in the experiment.

Using similar procedures, six types of samples, labeled Samples A–F, were prepared as shown in Figure 4, which indicates the heating process for each sample. Sample B (Figure 4b) corresponds to the sample shown in Figure 2. Sample A (Figure 4a) is a sample in which only the foaming and reheating of the precursor shown in Figure 2a–c were performed, while the roller forming shown in Figure 2d,e was not performed. Sample D (Figure 4d) was processed as follows: After reheating and performing the roller traverse once, it was cooled sufficiently to room temperature. Then, it was reheated to 630 °C, the roller was lowered by 2 mm, the roller traverse was performed once again, and it was cooled again to room temperature. This process was repeated until a total indentation depth of 10 mm was achieved. Sample C (Figure 4c) was subjected to six cycles of reheating and cooling without forming in Sample D. Sample F (Figure 4f) was subjected to the roller forming shown in Figure 2d,e immediately after foaming the precursor before cooling below the liquidus temperature. Sample E (Figure 4e) was subjected only to foaming the precursor. In this study, we prepared four samples for Sample A, eight samples for Sample B, four samples for Sample C, ten samples for Sample D, thirty samples for Sample E, and seven samples for Sample F.

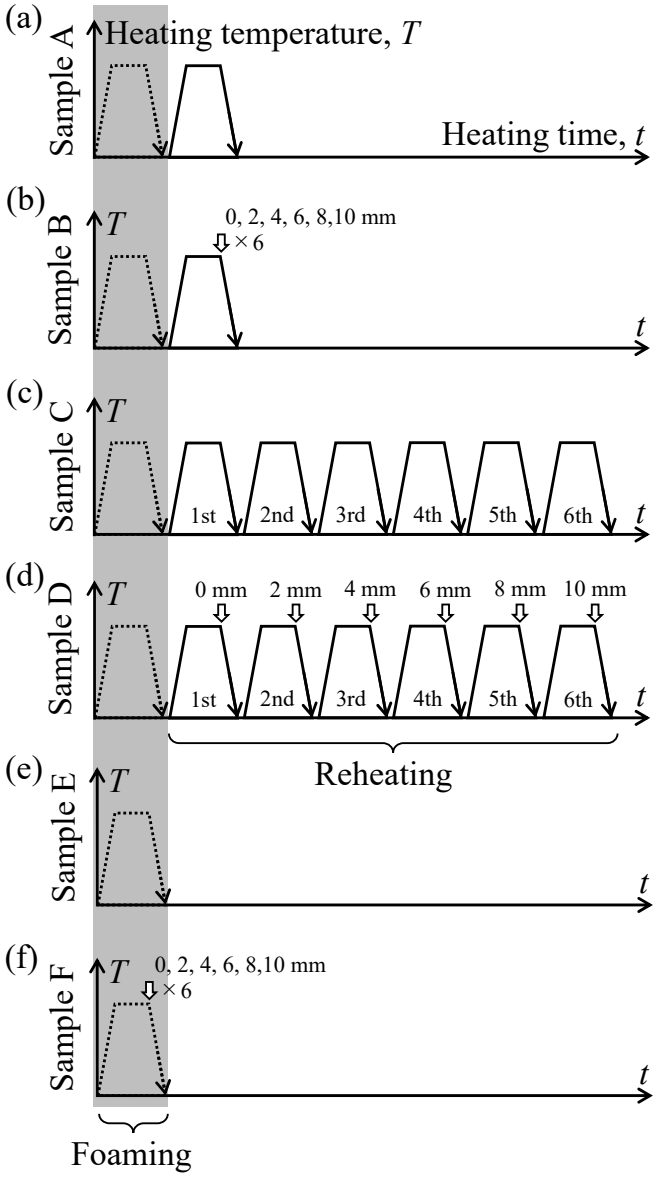


Figure 4. Foaming and reheating conditions for Samples A–F.

2.3. Observation of Pore Structures

After the roller forming process, X-ray CT imaging was performed on the obtained aluminum foam to observe the pore structures. Imaging was performed at an X-ray tube voltage of 80 kV and an X-ray tube current of 30 μA, with a pixel equivalent length of approximately 100–120 μm/pixel. The porosity p of the aluminum foam was calculated by Equation (1).

$$p = \frac{\rho_i - \rho_f}{\rho_i} \times 100, \quad (1)$$

where ρ_f is the density of the obtained aluminum foam evaluated by Archimedes' principle [47,53], and ρ_i is the density of the precursor before foaming. ρ_i was determined using the density of dense ADC12, as referred to in ref. [51].

3. Results and Discussion

Figure 5 shows the heating process of Sample A. Figure 5a–c shows the initial heating process during the foaming of the precursor. In addition, the lower section re-shows the extracted part of Sample A from Figure 4. Figure 5a shows the state immediately after starting heating of the precursor, and Figure 5b shows the state just before the precursor foamed and heating was stopped. The precursor exhibited significant foaming when heated. Figure 5c shows the state after heating was stopped, and the obtained aluminum foam was cooled below the liquidus temperature. Although slight shrinkage due to cooling was observed, aluminum foam was successfully fabricated. The measured porosity of this aluminum foam after cooling to room temperature was 81.0%. Figure 6 shows the relationship between temperature T and time t elapsed since heating began. Heating caused the temperature increase, but as it reached the solidus temperature, the temperature gradient became gradual, resulting in a solid–liquid coexistence state. At this point, the precursor began to foam. Then, once the temperature exceeded the liquidus temperature, the temperature gradient increased again, causing significant foaming. After stopping heating at 630 °C, the temperature continued to increase due to the residual heat, but cooling began shortly thereafter. For samples subjected to roller forming, forming was performed after the temperature reached 630 °C again. Subsequently, the temperature of the aluminum foam followed a reverse temperature history to that during heating, and similarly, the temperature gradient became gradual when the temperature reached the solid–liquid coexistence state.

Figure 5d–f shows the process of reheating the obtained aluminum foam, which was once cooled, as shown in Figure 5c, up to the same temperature applied for foaming. Figure 5d shows the state immediately after starting heating, and Figure 5e shows the state just before reaching 630 °C and stopping heating. No significant changes were observed during heating. Figure 5f shows the state after heating was stopped and the sample was cooled below the liquidus temperature. After heating stopped, slight shrinkage was observed. The porosity of this reheated aluminum foam after cooling to room temperature was 76.7%. Sample A was subjected to four trials. The average porosity of the as-foamed samples was 80.1%, whereas the average porosity of the reheated samples was 76.2%. That is, it was found that the aluminum foam slightly shrank when reheated. The reason for the slight shrinkage of the aluminum foam after reheating is considered as follows. Immediately after the foaming of the precursor, the pores maintained internal pressure due to the generated gas. Therefore, even as the aluminum foam cooled and shrank during solidification, the pores maintained their shape, resulting in no significant reduction in porosity. However, tiny holes formed in the cell wall during this solidification shrinkage [54–56]. In addition, previous research has indicated that heating causes the internal pressure of the gas to become equivalent to that during foaming [39]. Furthermore, it has been demonstrated

that the foaming agent in the precursor does not completely decompose after foaming; it remains within the aluminum foam and can generate gas through reheating [57]. When aluminum foam was reheated, gas was generated from the residual foaming agent during reheating. However, it is considered that the gas leaked through tiny holes in the cell walls and did not reach a sufficient internal pressure to be retained. Therefore, no expansion occurred during reheating, and it exhibited greater solidification shrinkage during cooling than immediately after foaming.

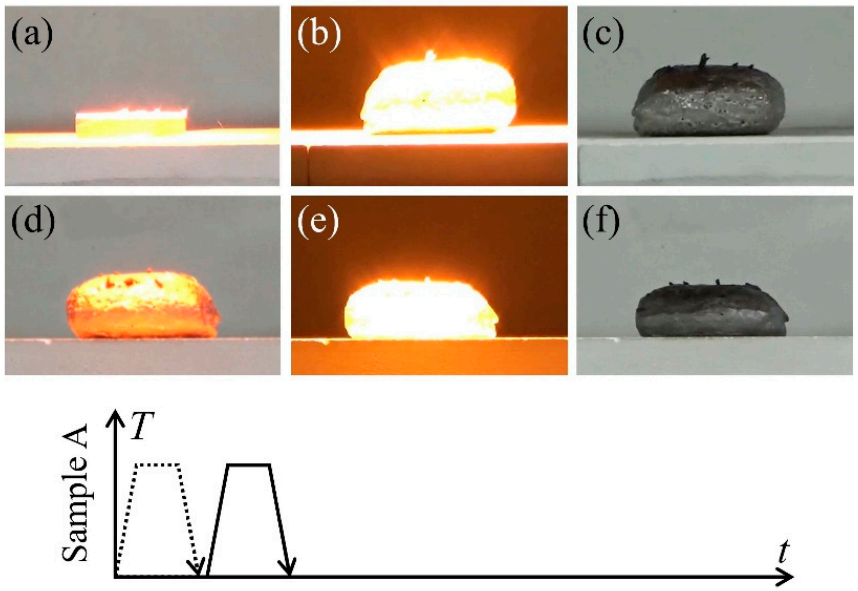


Figure 5. Heating process of Sample A: (**a**–**c**) Initial heating process during the foaming of the precursor; (**d**–**f**) reheating process of aluminum foam obtained in Figure 5c.

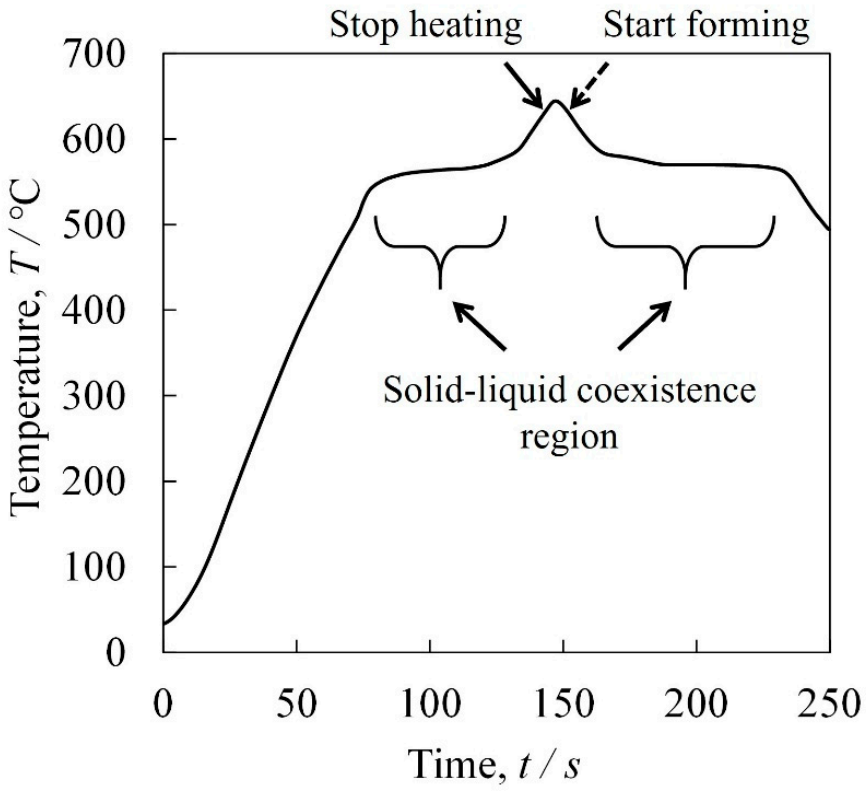


Figure 6. Relationship between temperature and time elapsed since heating began.

Figure 7a,b show the appearance of Samples C and E, and Figure 7c,d show X-ray CT images of Samples C and E. In the X-ray CT images, the white areas indicate the ADC12 region, while the black areas indicate pores or background air. Numerous pores were observed in both samples. The porosity of Sample C was slightly lower than that of as-foamed Sample E, but the X-ray CT images showed no evidence of localized shrinkage in any specific areas through reheating. Sample C exhibited an average porosity of 75.9% for four trials, while Sample E exhibited an average porosity of 80.0% for thirty trials.

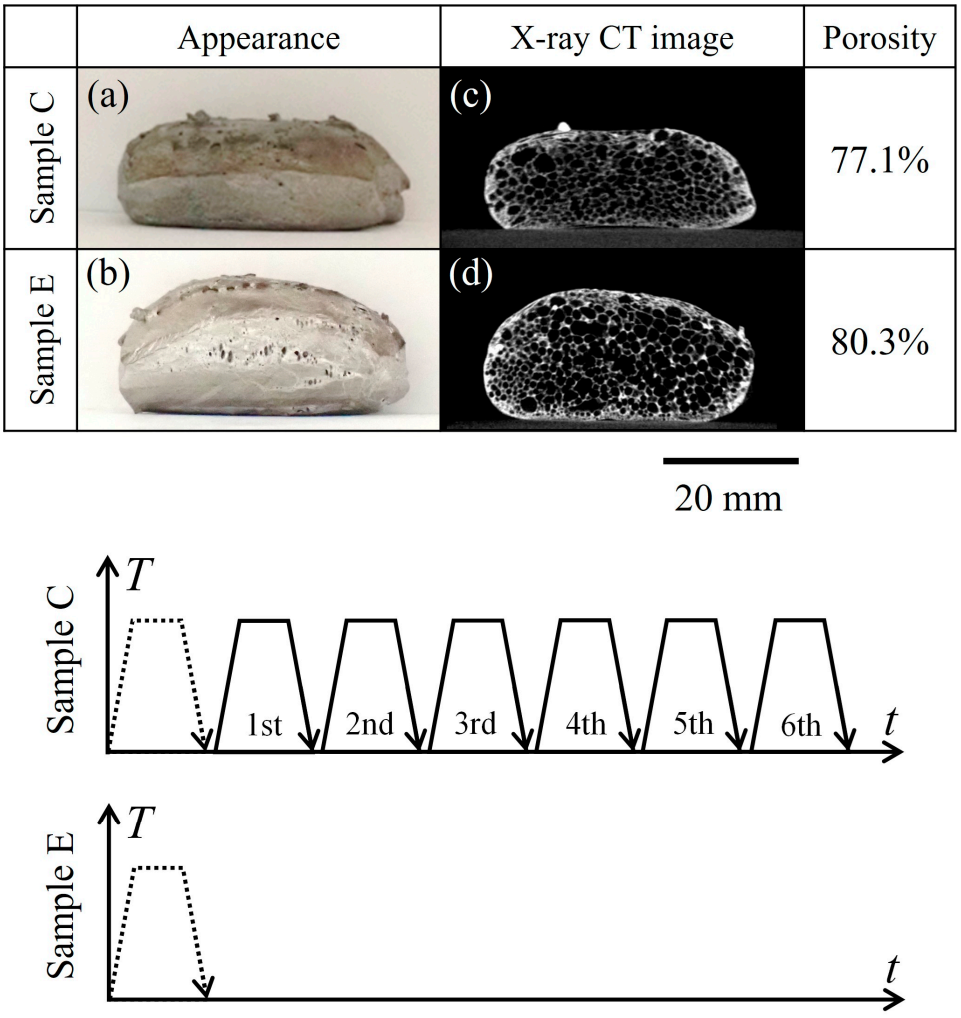


Figure 7. Appearances and X-ray CT images of Samples C and E.

Figure 8 shows the appearance observed from the top surface (the surface contacted by the roller) (Figure 8a–g), the appearance observed from the side (Figure 8h–n), and the cross-sectional X-ray CT images (Figure 8o–u) for the as-foamed sample and the samples subjected to reheating and roller forming, respectively, in Sample D, along with their porosities. The upper surface of the aluminum foam, where the roller contacted, was formed into a flat shape. As the roller indentation depth increased, flat-shaped aluminum foam with corresponding thicknesses can be fabricated. Consequently, it was found that aluminum foam that was initially foamed in a mountain shape can be formed into a flat shape. However, the porosity gradually decreased, and X-ray CT images showed an increase in white ADC12 areas, particularly on the upper layer near the surface, suggesting that the pores were slightly deformed and collapsed. However, despite the thickness of the aluminum foam with an indentation depth of 10 mm (6th) being equivalent to that of the initial precursor before foaming, its porosity still remained approximately 65%. That is,

not all pores were collapsed; instead, many pores were maintained, and the decrease in porosity was limited to about 15% compared to the as-foamed aluminum foam.

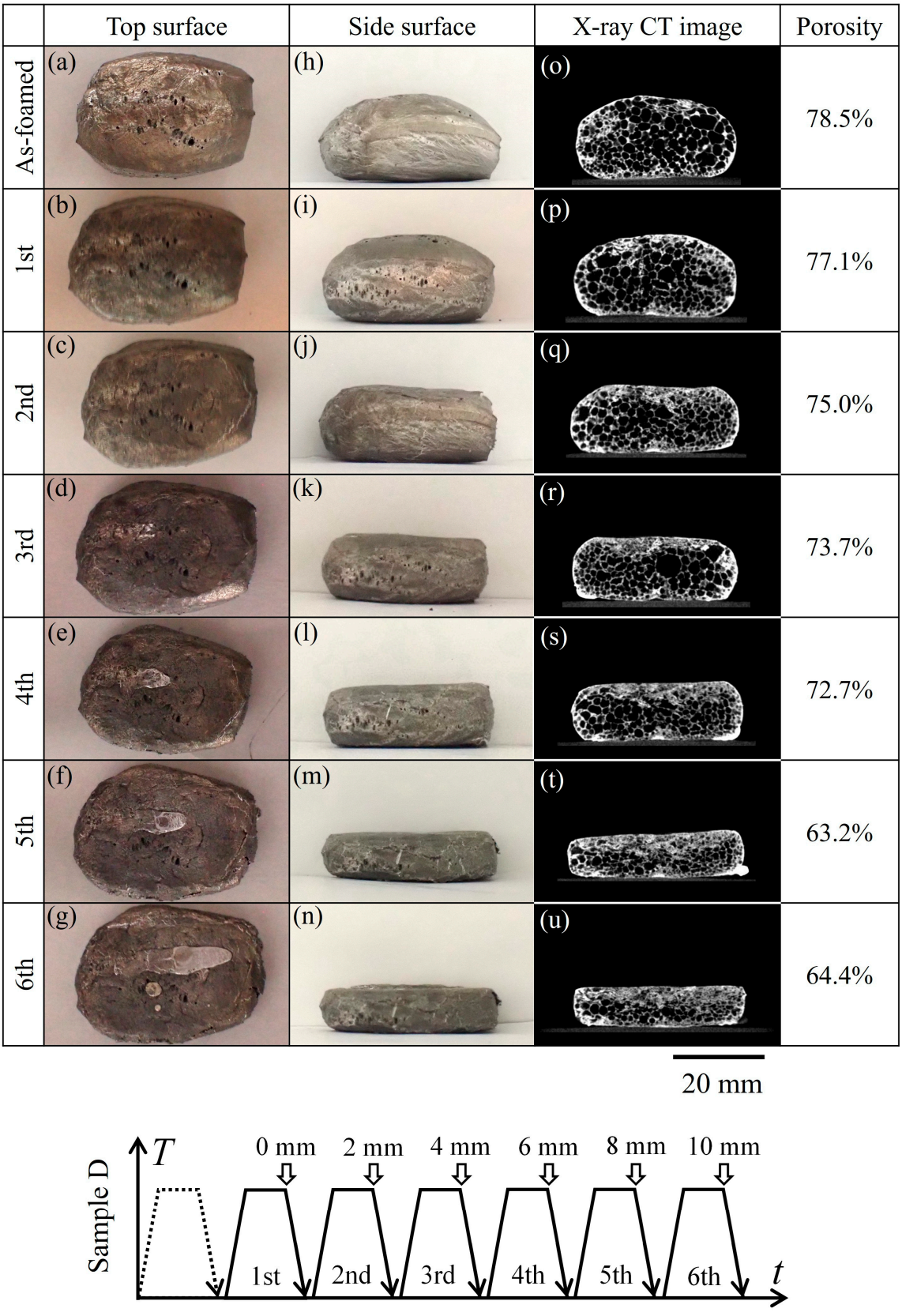


Figure 8. Appearances and X-ray CT images of Sample D.

Figure 9 shows the average porosity of as-foamed aluminum foam for Samples C and D, as well as aluminum foam after each reheating and roller forming cycle. First, in Sample C, when the as-foamed aluminum foam was reheated once, shrinkage occurred, as shown in Figure 5. However, after first reheating, no decrease in porosity occurred, even after repeated reheating and cooling. As described in Figure 5, this is considered to be due to the formation of tiny holes on the cell walls, allowing gas within the pores to freely escape, causing the ADC12 that constitutes the cell walls only to repeat thermal expansion and shrinkage through cooling. In contrast, in Sample D, the porosity gradually decreased with each reheating and roller forming process, and the difference in porosity compared to Sample C increased with each repeated reheating and roller forming cycle. Therefore, a decrease in porosity was considered to be caused by roller forming. Unlike the case of Sample F described later, the gas within the pores of reheated aluminum foam escaped, resulting in no internal pressure. This caused some pores to deform and collapse during the roller forming.

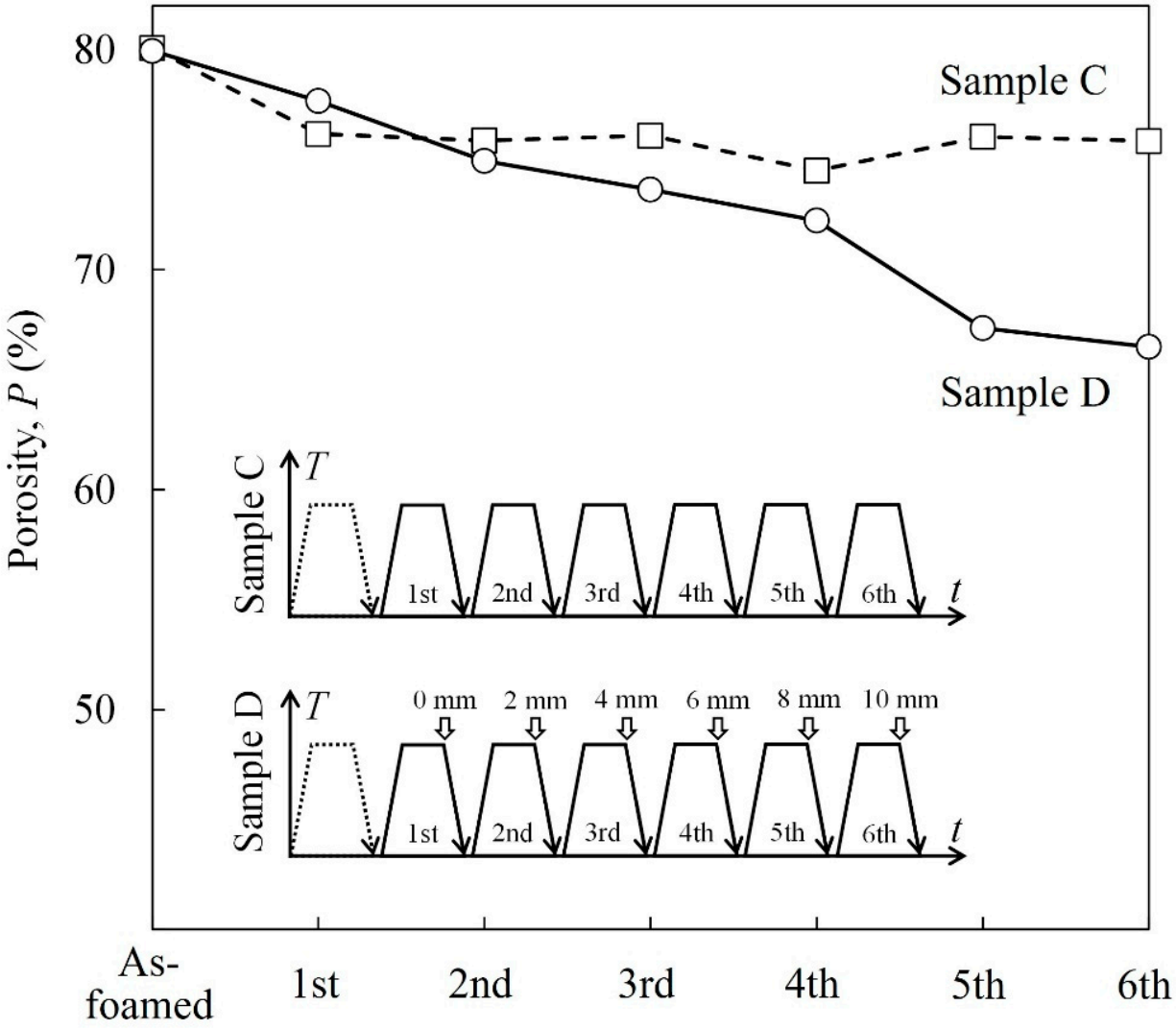


Figure 9. Porosity of as-foamed aluminum foam for Samples C and D, as well as aluminum foam after each reheating and roller forming cycle.

Figure 10 shows the appearance observed from the top surface (the surface contacted by the roller) (Figure 10a–c), the appearance observed from the side (Figure 10d–f), the X-ray CT cross-sectional images near the center (Figure 10g–i), and the porosities of Samples

B, D, and F. In all samples, the aluminum foam that was initially foamed into a mountain shape can be formed into a flat shape without any cracks or other defects appearing on the surface. However, in Samples B and D, compared to Sample F, even after roller forming, the expansion of aluminum foam in the lateral (circumferential) direction was low, and the porosity also decreased. This is considered to be the gradual deformation and collapsing of pores by the roller forming, as was also observed in Figure 9. This was also observed in the X-ray CT images, with Samples B and D showing an increase in white ADC12 areas, particularly on the upper layer near the surface, indicating partial deformation and collapsing of pores. Furthermore, for Sample D at the fourth roller forming, although aluminum foam was heated to 660 °C before roller forming, two out of ten samples could not be formed. At the sixth roller forming, the number of samples that cannot be formed increased to five out of ten. This is attributed to the repeated reheating causing the oxide layer on the surface skin layer to thicken and harden, and the robot arm used in this study was insufficient in forming force. However, it is presumed that forming performed using a robot arm with a high forming force would lead to crack formation on the surface. In Sample F, although buckling occurred at the right edge, it was possible to form it into a flat plate. The reason for the buckling was that at an indentation depth of 10 mm (sixth), the aluminum foam began to adhere to the roller, causing the right edge to lift. X-ray CT images of Sample F showed pores observed throughout the entire aluminum foam. However, at the top of the aluminum foam, a slightly white area was observed where the surface skin layer, which had initially foamed into a mountain shape, was folded due to being formed into a flat shape. In addition, Sample F was expanded in the circumferential direction more significantly than Samples B and D. The porosity of Sample F was also about 10% higher than that of Samples B and D, indicating a higher pore stability during forming. Thus, it was apparent that the aluminum foam of Sample F can form while maintaining its pores.

Figure 11 shows the average and standard deviation of the porosity for all samples. First, the cases without roller forming (Samples A, C, and E) were compared. It was shown that reheating caused a slight decrease in porosity, resulting in Samples A and C having a lower porosity than the as-foamed Sample E, as also shown in Figure 5. In contrast, Samples A and C exhibited similar porosities. Consequently, it was found that repeated reheating had no effect on the porosity, as also shown in Figure 9. Next, the roller-formed samples (Samples B, D, and F) were compared. Samples B and D exhibited similar porosities, both approximately 75%. This indicates that whether aluminum foam was formed with an indentation depth of 10 mm with only one reheating cycle or formed with an indentation depth of 10 mm by repeatedly reheating and roller forming every 2 mm, the porosity was not significantly affected. This indicates that when reheated and roller-formed, pores were deformed and collapsed, corresponding to the amount of thickness reduction. In addition, comparing Samples E and F, the porosities were slightly decreased by roller forming. This is considered to be because, as also shown in Figure 10, when the surface of the mountain-shaped aluminum foam was roller-formed, the thin skin layer on the surface was folded, resulting in the formation of a slightly thin dense layer near the surface. Furthermore, comparing Samples B and D with Sample F, it is apparent that roller forming immediately after foaming the precursor minimized the influence on the porosity. In Samples B and D, although the porosities were slightly decreased, they retained a significant number of pores. Consequently, although there was a slight decrease in porosities and influences on the pore structures, it was demonstrated that aluminum foam can be formed into a flat plate.

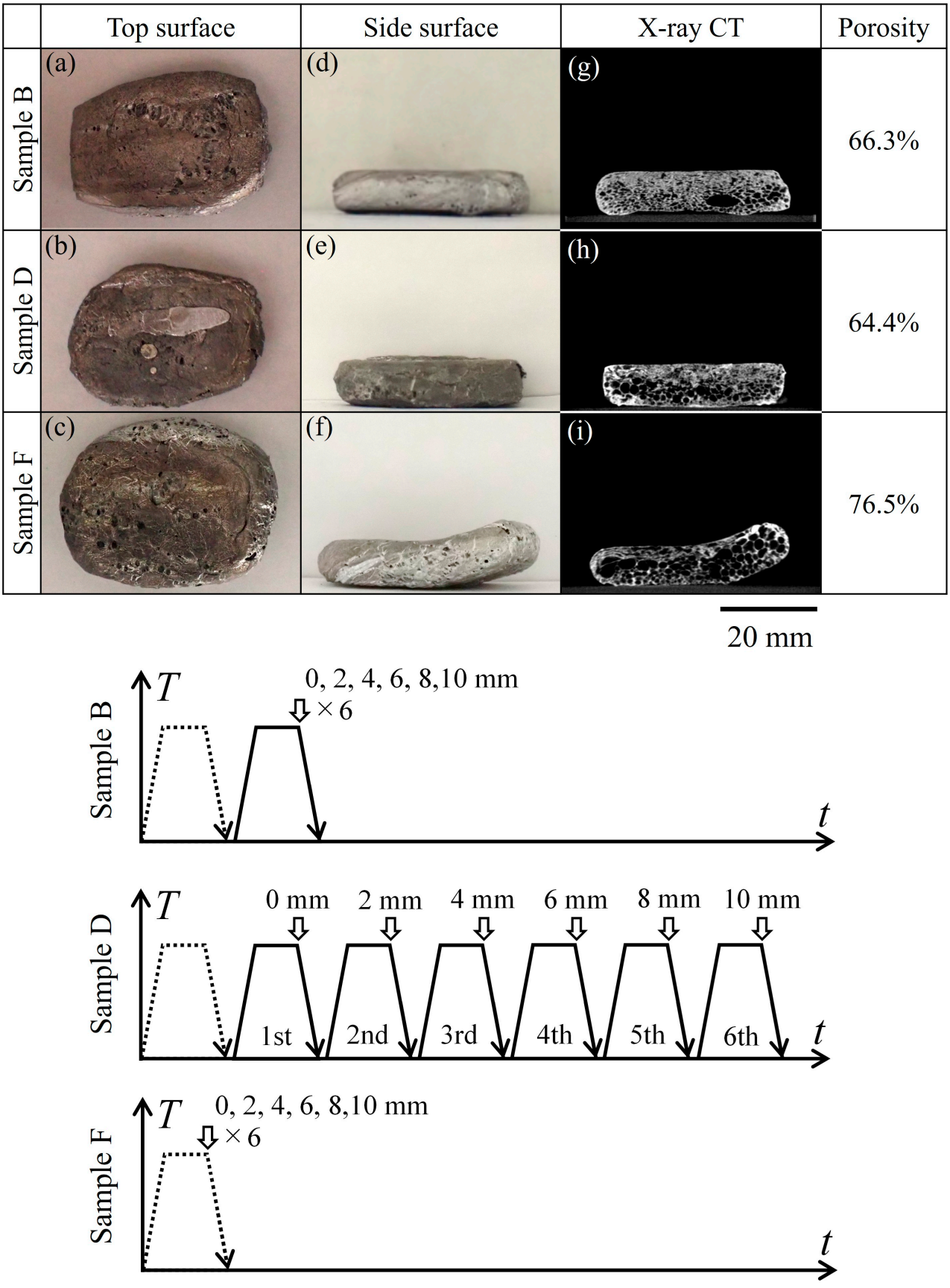


Figure 10. Appearances and X-ray CT images of Samples B, D, and F.

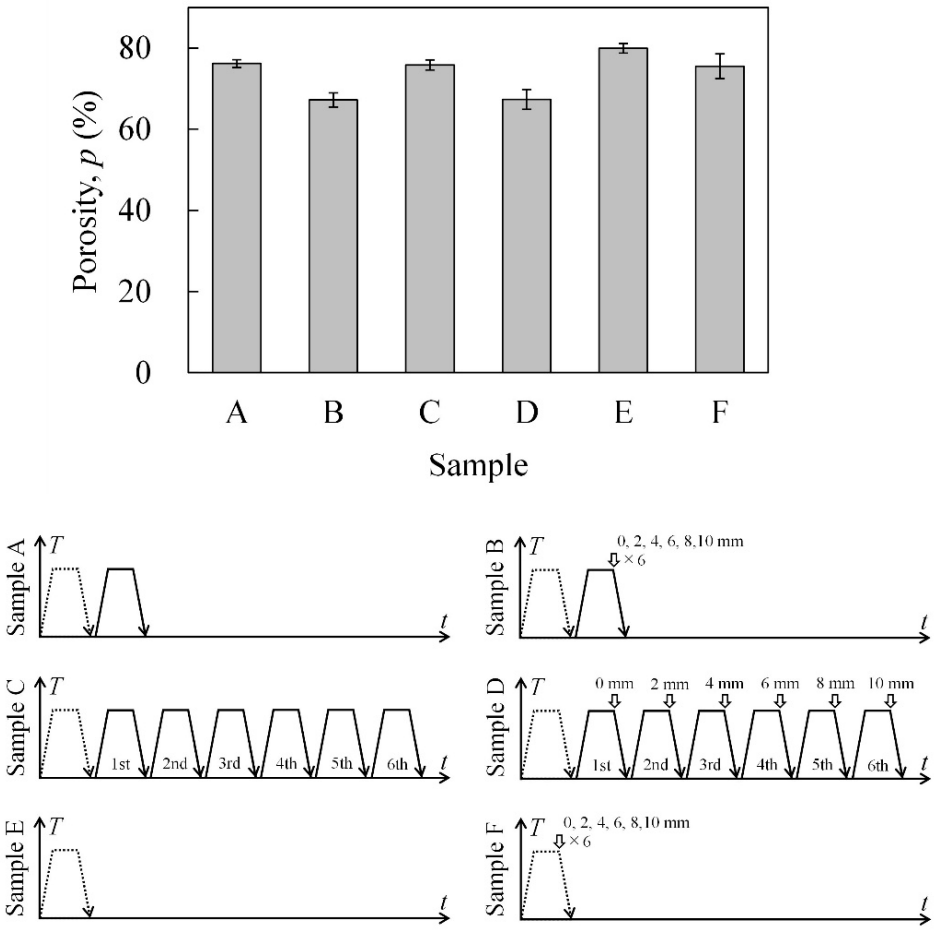


Figure 11. Averages and standard deviations of the porosities for all samples investigated in this study.

4. Conclusions

In this study, we attempted to form aluminum foam, which was fabricated by heating and foaming a precursor, into a flat plate by reheating it above its liquidus temperature and then roller forming it. The following results were obtained.

(1) Aluminum foam tended to shrink slightly with reheating, but not significantly. X-ray CT images showed no evidence of shrinkage in any particular areas by reheating.

(2) The shrinkage by reheating occurred during the initial reheating, and a slight decrease in porosity was observed. In contrast, it was found that subsequent cycles of reheating and cooling had no effect on the porosity. However, from the perspective of formability, it was found that under the conditions set in this study, the high hardness of the aluminum foam surface, presumed to be caused by the thickening of the oxide film, limits the number of reheating and cooling cycles to approximately three.

(3) In all samples, heating above the liquidus temperature and roller forming enabled the aluminum foam, which had foamed into a mountain shape, to be formed into a flat plate without causing cracks on the surface.

(4) In Sample F, in which the precursor was roller-formed immediately after foaming, it was found that compared to the as-foamed Sample E, the decrease in porosity was limited to approximately 5%, enabling roller forming while minimizing the influences on pore structures.

(5) In Samples B and D, which were roller-formed after reheating, the porosities decreased, but most pores were retained. Even when the aluminum foam was roller-formed to the same thickness as the initial precursor before foaming, the porosities exhibited

around 65%, limiting the reduction in porosities to approximately 15% compared to the as-foamed aluminum foam.

(6) Whether the roller forming was performed gradually through repeated reheating and roller forming, or all at once after reheating, similar porosities, both approximately 75%, were obtained if the indentation depth was the same.

Author Contributions: Conceptualization, Y.H., K.I. and K.A.; methodology, K.I.; validation, Y.H. and K.I.; formal analysis, K.I.; investigation, K.I.; resources, N.Y.; data curation, Y.H. and K.I.; writing—original draft preparation, Y.H. and K.I.; writing—review and editing, K.A.; visualization, K.I. and N.Y. All authors have read and agreed to the published version of the manuscript.

Funding: This research was financially supported partly by the Light Metal Education Foundation and the Amada Foundation.

Data Availability Statement: The original contributions presented in this study are included in the article. Further inquiries can be directed to the corresponding author.

Conflicts of Interest: The authors declare no conflicts of interest.

References

1. Gibson, L.J. Mechanical behavior of metallic foams. *Annu. Rev. Mater. Sci.* **2000**, *30*, 191–227. [CrossRef]
2. Ji, C.; Huang, H.; Wang, T.; Huang, Q. Recent advances and future trends in processing methods and characterization technologies of aluminum foam composite structures: A review. *J. Manuf. Process.* **2023**, *93*, 116–152. [CrossRef]
3. Wang, E.D.; Yao, R.Y.; Li, Q.; Hu, X.Y.; Sun, G.Y. Lightweight metallic cellular materials: A systematic review on mechanical characteristics and engineering applications. *Int. J. Mech. Sci.* **2024**, *270*, 55. [CrossRef]
4. Neu, T.R.; Heim, K.; Seeliger, W.; Kamm, P.H.; García-Moreno, F. Aluminum Foam Sandwiches: A Lighter Future for Car Bodies. *JOM* **2024**, *76*, 2619–2630. [CrossRef]
5. Fu, W.; Li, Y. Fabrication, Processing, Properties, and Applications of Closed-Cell Aluminum Foams: A Review. *Materials* **2024**, *17*, 560. [CrossRef]
6. Kumai, S. Role and Potential of Aluminium and Its Alloys for a Zero-Carbon Society. *Mater. Trans.* **2023**, *64*, 319–333. [CrossRef]
7. Krall, P.; Weißensteiner, I.; Pogatscher, S. Recycling aluminum alloys for the automotive industry: Breaking the source-sink paradigm. *Resour. Conserv. Recycl.* **2024**, *202*, 107370. [CrossRef]
8. Kathuria, Y.P. A preliminary study on laser assisted aluminum foaming. *J. Mater. Sci.* **2003**, *38*, 2875–2881. [CrossRef]
9. Guglielmotti, A.; Quadrini, F.; Squeo, E.A.; Tagliaferri, V. Laser bending of aluminum foam sandwich panels. *Adv. Eng. Mater.* **2009**, *11*, 902–906. [CrossRef]
10. Quadrini, F.; Guglielmotti, A.; Squeo, E.A.; Tagliaferri, V. Laser forming of open-cell aluminium foams. *J. Mater. Process. Technol.* **2010**, *210*, 1517–1522. [CrossRef]
11. Yilbas, B.S.; Akhtar, S.S.; Keles, O. Laser hole cutting in aluminum foam: Influence of hole diameter on thermal stress. *Opt. Lasers Eng.* **2013**, *51*, 23–29. [CrossRef]
12. Contorno, D.; Filice, L.; Fratini, L.; Micari, F. Forming of aluminum foam sandwich panels: Numerical simulations and experimental tests. *J. Mater. Process. Technol.* **2006**, *177*, 364–367. [CrossRef]
13. Gagliardi, F.; Filice, L.; Umbrello, D.; Shivpuri, R. Forging of metallic foams to reproduce biomechanical components. *Mater. Sci. Eng. A* **2008**, *480*, 510–516. [CrossRef]
14. Cai, Z.-Y.; Zhang, X.; Liang, X.-B. Multi-point forming of sandwich panels with egg-box-like cores and failure behaviors in forming process: Analytical models, numerical and experimental investigations. *Mater. Des.* **2018**, *160*, 1029–1041. [CrossRef]
15. Zhang, W.; Cai, Z.; Zhang, X.; Gao, J.; Wang, M.; Chen, Q. Numerical Simulation Analysis on Surface Quality of Aluminum Foam Sandwich Panel in Plastic Forming. *Metals* **2023**, *13*, 65. [CrossRef]
16. Nassar, H.; Albakri, M.; Pan, H.; Khraisheh, M. On the gas pressure forming of aluminium foam sandwich panels: Experiments and numerical simulations. *CIRP Ann.* **2012**, *61*, 243–246. [CrossRef]
17. Mata, H.; Santos, A.D.; Parente, M.P.L.; Valente, R.A.F.; Fernandes, A.A.; Jorge, R.N. Study on the forming of sandwich shells with closed-cell foam cores. *Int. J. Mater. Form.* **2014**, *7*, 413–424. [CrossRef]
18. Jackson, K.P.; Allwood, J.M.; Landert, M. Incremental forming of sandwich panels. *J. Mater. Process. Technol.* **2008**, *204*, 290–303. [CrossRef]
19. Matsumoto, R.; Tsuruoka, H.; Otsu, M.; Utsunomiya, H. Fabrication of skin layer on aluminum foam surface by friction stir incremental forming and its mechanical properties. *J. Mater. Process. Technol.* **2015**, *218*, 23–31. [CrossRef]

20. Kim, W.Y.; Kim, W.J.; Utsunomiya, H. Accelerated Formation of an Ultrafine-Grained Microstructure in Closed-Cell Aluminum Foam after Extrusion and Differential Speed Rolling. *Mater. Trans.* **2017**, *58*, 291–293. [CrossRef]
21. Weiss, M.; Abeyrathna, B.; Pereira, M. Roll formability of aluminium foam sandwich panels. *Int. J. Adv. Manuf. Technol.* **2018**, *97*, 953–965. [CrossRef]
22. Miyoshi, T.; Itoh, M.; Akiyama, S.; Kitahara, A. ALPORAS aluminum foam: Production process, properties, and applications. *Adv. Eng. Mater.* **2000**, *2*, 179–183. [CrossRef]
23. Banhart, J. Manufacture, characterisation and application of cellular metals and metal foams. *Prog. Mater. Sci.* **2001**, *46*, 559–632. [CrossRef]
24. Banhart, J. Light-Metal Foams—History of Innovation and Technological Challenges. *Adv. Eng. Mater.* **2013**, *15*, 82–111. [CrossRef]
25. García-Moreno, F. Commercial applications of metal foams: Their properties and production. *Materials* **2016**, *9*, 85. [CrossRef]
26. Patel, N.; Mittal, G.; Agrawal, M.; Pradhan, A.K. Aluminum foam production, properties, and applications: A review. *Int. J. Met.* **2024**, *18*, 2181–2198. [CrossRef]
27. Baumgartner, F.; Duarte, I.; Banhart, J. Industrialization of powder compact foaming process. *Adv. Eng. Mater.* **2000**, *2*, 168–174. [CrossRef]
28. Kanetake, N.; Kobashi, M.; Tsuda, S. Foaming Behavior of Aluminum Precursor Produced from Machined Chip Waste. *Adv. Eng. Mater.* **2008**, *10*, 840–844. [CrossRef]
29. Duarte, I.; Vesenjak, M.; Vide, M.J. Automated Continuous Production Line of Parts Made of Metallic Foams. *Metals* **2019**, *9*, 531. [CrossRef]
30. Yuan, G.; Li, Y.; Zhou, X.; Hu, L. Preparation of complex shaped aluminum foam by a novel casting-foaming method. *Mater. Lett.* **2021**, *293*, 129673. [CrossRef]
31. Guo, Z.; Feng, Z.; Zu, G.; Yuan, X.; Wang, F. Foaming Behavior of AlSi8Mg4 Alloy in Closed Cavity. *Int. J. Met.* **2023**, *17*, 947–958. [CrossRef]
32. Duarte, I.; Banhart, J. A study of aluminium foam formation—Kinetics and microstructure. *Acta Mater.* **2000**, *48*, 2349–2362. [CrossRef]
33. Hangai, Y.; Takada, K.; Fujii, H.; Aoki, Y.; Aihara, Y.; Nagahiro, R.; Amagai, K.; Utsunomiya, T.; Yoshikawa, N. Foaming of A1050 aluminum precursor by generated frictional heat during friction stir processing of steel plate. *Int. J. Adv. Manuf. Technol.* **2020**, *106*, 3131–3137. [CrossRef]
34. Hangai, Y.; Ohashi, M.; Nagahiro, R.; Amagai, K.; Utsunomiya, T.; Yoshikawa, N. Press forming of aluminum foam during foaming of precursor. *Mater. Trans.* **2019**, *60*, 2464–2469. [CrossRef]
35. Hangai, Y.; Kawato, D.; Ando, M.; Ohashi, M.; Morisada, Y.; Ogura, T.; Fujii, H.; Nagahiro, R.; Amagai, K.; Utsunomiya, T.; et al. Nondestructive observation of pores during press forming of aluminum foam by X-ray radiography. *Mater. Charact.* **2020**, *170*, 110631. [CrossRef]
36. Hangai, Y.; Sakaguchi, Y.; Okada, K.; Tanaka, Y. Press-forming of aluminum foam and estimation of its mechanical properties from X-ray CT images using machine learning. *Mater. Charact.* **2025**, *221*, 114781. [CrossRef]
37. Hangai, Y.; Suzuki, K.; Ohashi, M.; Mitsugi, H.; Amagai, K. Roll forming of aluminum foam immediately after precursor foaming. *Results Eng.* **2021**, *10*, 100224. [CrossRef]
38. Liu, Z.-Y.; Cheng, Y.; Li, Y.-X.; Zhou, X.; Chen, X.; Wang, N.-Z. Shape formation of closed-cell aluminum foam in solid–liquid–gas coexisting state. *Int. J. Miner. Metall. Mater.* **2018**, *25*, 974–980. [CrossRef]
39. Liu, Z.; Cheng, Y.; Li, Y.; Wang, N.; Zhou, X. Study on Deformation of Closed-Cell Aluminum Foam in Different Solid–Liquid–Gas Coexisting State. *Met. Mater. Int.* **2021**, *27*, 403–412. [CrossRef]
40. Movahedi, N.; Linul, E.; Marsavina, L. The Temperature Effect on the Compressive Behavior of Closed-Cell Aluminum-Alloy Foams. *J. Mater. Eng. Perform.* **2018**, *27*, 99–108. [CrossRef]
41. Hangai, Y.; Utsunomiya, T.; Hasegawa, M. Effect of tool rotating rate on foaming properties of porous aluminum fabricated by using friction stir processing. *J. Mater. Process. Technol.* **2010**, *210*, 288–292. [CrossRef]
42. Papantoniou, I.G.; Manolakos, D.E. Fabrication and characterization of aluminum foam reinforced with nanostructured γ-Al_2O_3 via friction stir process for enhanced mechanical performance. *Int. J. Adv. Manuf. Technol.* **2024**, *130*, 5359–5368. [CrossRef]
43. Lohani, D.; Dhanish, S.; Daniel, B.S.S. Modelling and optimization of experimental parameters for porosity in friction stir processed aluminum foam using response surface methodology. *Adv. Mater. Process. Technol.* **2024**, *11*, 2436–2456. [CrossRef]
44. Zhang, Y.; Pang, Q. Study on the Process of Preparing Aluminum Foam Sandwich Panel Precursor by Friction Stir Welding. *Materials* **2024**, *17*, 4981. [CrossRef]
45. Lohani, D.; Daniel, B.S.S. Quasi-static Deformation Mechanism and Compressive Properties of Aluminum Foams Fabricated by Friction Stir Processing. *J. Mater. Eng. Perform.* **2025**, *34*, 5072–5080. [CrossRef]
46. Alizadeh, E.; Mashtizadeh, A.R.; Azizieh, M. Influence of Titanium Hydride Heat Treatment Time on Pore Morphology of Friction Stir Welded Aluminum Nanocomposite Foams. *Trans. Indian Inst. Met.* **2025**, *78*, 254. [CrossRef]

47. Mishra, S.; Mouria, P.K.; Bhardwaj, P.; Mehdi, H. Optimization of friction stir processing parameters using RSM and their impact on the mechanical characteristics of AA6063 metal foam. *Int. J. Interact. Des. Manuf. (IJIDeM)* **2026**, *20*, 407–423. [CrossRef]
48. *JIS-H-2118*; Aluminium Alloy Ingots for Die Castings. Japanese Standards Association: Tokyo, Japan, 2006.
49. *JIS-H-5302*; Aluminium Alloy Die Castings. Japanese Standards Association: Tokyo, Japan, 2006.
50. Hangai, Y.; Kaneko, Y.; Amagai, K. Continuous Fabrication Process of Aluminum Foam from Foaming to Press Forming. *Metals* **2025**, *15*, 633. [CrossRef]
51. The-Japan-Institute-of-Light-Metals. *Structures and Properties of Aluminum*; The Japan Institute of Light Metals: Tokyo, Japan, 1991.
52. Ishiuchi, K.; Hangai, Y.; Amagai, K.; Yoshikawa, N.; Ogura, T.; Morisada, Y.; Fujii, H. ADC12 Porous Aluminum Shape Formation via Multi-Stage Roller Forming. *J. Rep. Jpn. Foundry Eng. Soc. Meet.* **2024**, *183*, 29. [CrossRef]
53. Lohani, D.; Daniel, B.S.S. Influence of Al_2O_3 Additives on Mechanical Properties and Energy Absorption in Closed-Cell Aluminum Foam Fabricated via Friction Stir Processing. *Trans. Indian Inst. Met.* **2025**, *78*, 83. [CrossRef]
54. Jeon, I.; Asahina, T. The effect of structural defects on the compressive behavior of closed-cell Al foam. *Acta Mater.* **2005**, *53*, 3415–3423. [CrossRef]
55. Mukherjee, M.; Garcia-Moreno, F.; Banhart, J. Defect generation during solidification of aluminium foams. *Scr. Mater.* **2010**, *63*, 235–238. [CrossRef]
56. Lázaro, J.; Solórzano, E.; Rodríguez-Pérez, M.A.; Kennedy, A.R. Effect of solidification rate on pore connectivity of aluminium foams and its consequences on mechanical properties. *Mater. Sci. Eng. A* **2016**, *672*, 236–246. [CrossRef]
57. Hangai, Y.; Takagi, T.; Koyama, S.; Suzuki, R.; Kamakoshi, Y. Refoaming of deformed aluminum foam fabricated by precursor foaming process using remaining foaming agent and densification using friction stir welding. *Mater. Lett.* **2023**, *351*, 135008. [CrossRef]

Disclaimer/Publisher's Note: The statements, opinions and data contained in all publications are solely those of the individual author(s) and contributor(s) and not of MDPI and/or the editor(s). MDPI and/or the editor(s) disclaim responsibility for any injury to people or property resulting from any ideas, methods, instructions or products referred to in the content.